Enhancing sustainability of household water filters by mixing metallic iron with porous materials

Noubactep C.[*(a,c)], Caré S.[(b)]

[(a)] Angewandte Geologie, Universität Göttingen, Goldschmidtstraße 3, D - 37077 Göttingen, Germany;

[(b)] Université Paris-Est, Laboratoire Navier, Ecole des Ponts - ParisTech, LCPC, CNRS, 2 allée Kepler, 77420 Champs sur Marne, France;

[(c)] Kultur und Nachhaltige Entwicklung CDD e.V., Postfach 1502, D - 37005 Göttingen, Germany.

* corresponding author: e-mail: cnoubac@gwdg.de; Tel. +49 551 39 3191, Fax: +49 551 399379

(Accepted: 08 Jun 2010)

Abstract: This study conceptually discusses the feasibility of enhancing the sustainability of conventional iron/sand filter (Fe^0/sand filter) for safe drinking water by partially or totally substituting sand (quartz) by porous materials. Relevant materials included activated carbon, dolomites, limestone, pumice, sandstone, and zeolites. The rational was to use the internal volume of porous additives as storage room for in-situ generated iron oxyhydroxides (iron corrosion products) and thus delay time to filter clogging. Based on previous works a filter with a volumetric Fe^0:quartz ratio of 51:49 was used as reference system. The reference system is clogged upon Fe^0 depletion. Results showed that totally substituting quartz by pumice particles having a porosity of 80 % yields to a residual porosity of 41 %. This encouraging result suggested that the possibility of using Fe^0/MnO_2/pumice systems for a synergic promotion of Fe^0 reactivity (by MnO_2) and filter permeability (by pumice) should be investigated in more details.

Keywords: Drinking water, Iron/sand filter; Long-term reactivity; Pumice; Zerovalent iron.

Capsule: Partially or totally replacing quartz by porous materials is a potential efficient tool to lengthen iron/sand filter service life.

1 Introduction

Safe drinking water is becoming worldwide an increasingly scarce resource mostly due to industrialization [1-3]. The situation is exacerbated in rural areas of the developing world where no centralized drinking water system is available. Therefore, efforts have been made to develop simple, efficient and affordable methods for safe drinking water production at household or small community level [4-9]. An ideal water treatment system for developing countries should remove all possible biological and chemical contaminants in a single-stage filtration process (Prerequisite 1). Only reverse osmosis membranes have been reported to achieve prerequisite 1. However, this high cost technology is not always affordable for the populations in need [1,10-12]. Therefore, efforts to develop simple, efficient and affordable filters (achieving prerequisite 1) for households and/or small communities is an area of ongoing active research [2,3,12-15].

In recent years, a great deal of work has been devoted at identifying suitable, low-cost, and readily available materials to be used in efficient household filters. Potential media include activated alumina, agricultural by-products (e.g. rice hulls), apatite, clay minerals, granular activated carbon (GAC), industrial by-products, iron-oxide (coated sands), manganese-oxide (coated sands), metallic iron (Fe^0), peat and peat moss, phosphate rocks, seaweeds and their derivatives, wood chips, and zeolites [2,3,16,17]. Some enumerated materials are regionally readily available (e.g. apatite, clay minerals, zeolites) at no-expense or at a fairly low cost. However, only metallic iron (Fe^0) is universally available. Next to its universally availability, the superiority of Fe^0 is justified by the fact that during the dynamic process of its aqueous oxidative dissolution (iron corrosion), several classes of biological and chemical contaminant can be removed from water [14,18-23]. In particular Fe^0 beds could quantitatively remove aqueous inorganic (e.g. Mo^{VI}) and organic (e.g. non-polar carboxylated organics) substances that are not readily removed by iron oxyhydroxides [24,25] Therefore, upon proper design, Fe^0 filters necessarily achieve prerequisite 1.

Ideally, a household filter should reduce contaminant concentrations to acceptable levels whilst retaining adequate permeability and reactivity over extended time periods (e.g. 12 months). Due to the volumetric expansive nature of iron corrosion [26-29], designing iron filters with long-term adequate permeability is a challenge for the scientific community [30]. In fact, very efficient Fe^0 filters (e.g. the 3-Kolshi filter) for safe drinking water have been tested in Bangladesh and Nepal for arsenic removal [31-34] but were abandoned because of service lives of only 6 to 24 weeks [35-37]. Hussam [37] reported that 3-Kolshi filters were "highly functional, but not sustainable" as the filters experienced permeability loss after 3 to 6 months. The alternative to 3-Kolshi filters was an improved filter called SONO filters [13,33,37]. The heart of SONO filters is a manufactured porous composite iron matrix (CIM). CIM is manufactured from Fe^0 and resulted filters could work for up to 11 years [37].

The present theoretical work is part of ongoing efforts, aiming at reviving conventional Fe^0 filters. The objective is to design efficient stand-alone Fe^0 filters for households and small communities. A recent article [30] has shown that mixing non porous sand (quartz) with Fe^0 is an efficient way to lengthen Fe^0 filter service live while saving up to the half amount of used Fe^0. It was shown that a filter with 51 vol-% Fe^0 necessarily has a longer service live than the conventional iron filter (100 % Fe^0), likely with the same efficiency. In the present work calculations will be made to access the possibility to further optimize filter efficiency by partly or entirely replacing quartz by porous materials. Relevant materials (Supporting Information) included activated carbon and natural minerals (e.g. MnO_2, TiO_2, zeolites) and rocks (e.g. dolomite, limestone, pumice, sandstone). For the sake of clarity, the Fe^0/sand/H_2O system will first be presented.

2 The Fe^0/sand/H_2O system

2.1 Descriptive aspects

Aqueous contaminant removal in the presence of Fe^0 (e.g. in Fe^0/H_2O systems) is an heterogeneous reaction ideally involving five steps: (i) contaminant mass-transfer from the

77 bulk solution to the Fe^0 surface, (ii) contaminant adsorption on the Fe^0 surface, (iii) chemical
78 reaction at the Fe^0 surface, (iv) desorption of the reaction products from Fe^0 surface, and (v)
79 mass-transfer of the reaction products into the bulk solution [38,39]. The kinetics of the
80 process of contaminant removal in a Fe^0/H_2O system are necessarily dependent on the
81 availability of the Fe^0 surface as well as the rate of mass-transfer of the contaminant to the
82 reactive Fe^0 surface (Fe^0 accessibility). Accordingly, mixing an inert material (e.g. sand) and
83 Fe^0 is coupled with a decrease of the contaminant removal rate as the pathway to the Fe^0
84 surface is lengthened (Assertion 1: mixing sand and Fe^0 decreases Fe^0 accessibility).
85 The process of aqueous iron oxidative dissolution at pH > 4.0 is characterized by the
86 expansive nature of iron corrosion products (iron oxides and oxyhydroxides or simply iron
87 oxyhydroxides). Depending on the nature of iron oxyhydroxide, a volumetric expansion of up
88 to 6.4 has been reported [28]. In other words, an iron oxyhydroxide molecule may occupy a
89 volume up to 6.4 times the volume of atomic Fe in the lattice structure. Accordingly, a pure
90 iron bed (100 % Fe^0) will clog sooner than a bed containing the same iron mixed with inert
91 material (e.g. sand). Therefore, mixing sand and Fe^0 should be regarded as a tool to sustain
92 permeability of an iron bed (Assertion 2: mixing sand and Fe^0 increases bed service life).
93 Assertion 1 and Assertion 2 clearly show that the role of sand in an Fe^0 bed is antagonistic.
94 Accordingly, a well-designed Fe^0/sand bed must conciliate limited Fe^0 accessibility and
95 extended service life. It is obvious that a critical volumetric Fe^0:sand ratio exists above which
96 bed clogging will occur upon Fe^0 depletion. That is the Fe^0 proportion for which in-situ
97 generated iron oxyhydroxides will fill the inter-granular pore volume of the initial bed. The
98 results of such calculations for the Fe^0:quartz is recalled in the next paragraph.

99 **2.2 Literature review**

100 Iron has been mixed with inert materials (including gravel and sand) since the early stage of
101 investigations regarding the applicability of iron walls for groundwater remediation [40,41].
102 However, there has been no systematic study designed to rationalize the effects of sand on the

efficiency of Fe^0 beds. Most researchers employ varying Fe^0:sand ratios for filtration beds in the laboratory and in the field on a pragmatic basis [42-48]. Fe^0:sand ratios are often given in weight percent without information on the available pore volume nor precise data on further operational conditions including the high of the Fe^0/sand bed (Table 1). As a result, controversial reports for the same systems have been reported. For example, while investigating As removal by Fe^0 in packed beds, Lien and Wilkin [46] concluded that Fe^0 alone performed better than a 50:50 sand:Fe^0 mixture. In contrary, Westerhoff et al. [47] observed higher As removal in a Fe^0:sand bed than with Fe^0 alone.

2.3 The importance of volumetric ratios

The main concern of available data on Fe^0/sand/H_2O systems is their comparability. When the Fe^0:sand ratios are given in percent it is not always specified whether it is volumetric or weight based. However, given the large difference between the density of sand (< 2,000 kg/m^3) and iron (7,800 kg/m^3), it should always explicitly said whether given percent are volumetric (vol-%) or weight (wt-%). Even in some cases (e.g. ref. [42]), the Fe^0:sand ratio is given without the high of the reactive zone nor the mass of either sand or iron.

2.3.1 Rationale for use the volumetric ratio

The sole calculation that could be founded to rationalize used Fe^0:sand ratios is given by Leupin et al. [45] and mentioned by Gottinger [15,49]. The authors used 2.5 g of Fe^0 which occupied a volume of 0.32 cm^3 and lead to 4.78 g of $Fe(OH)_3$ with a volume of 1.35 cm^3 (i.e. 4.78 cm^3 as reported in the original work). Then the internal porosity of sand (40 %) is considered to estimate the volume of sand necessary to contain the 1.35 cm^3 of iron oxides. Leupin et al. [45] came to the conclusion that at least 9.9 cm^3 (i.e. 35 cm^3) of sand should be used per gram of iron to avoid the clogging of more than a third of the void volume.

The calculus of Leupin et al. [45], considered as a rough estimate by the authors, has to be improved because they have not taken into account the inter-granular voids in the Fe^0/sand bed. In fact, the filter has to be considered as a granular medium with two types of porosity:

129 (i) the internal porosity of particle (as mentioned in ref. [45]) and (ii) the inter-granular voids
130 as a function of the compactness of the granular medium. A recent result [30] has allowed
131 modelling the clogging of Fe^0/quartz bed. Quartz is an inert, non porous material which can
132 not contribute to porosity loss. This modelling gives the evolution of the inter-granular void
133 as a function of the proportion of reactive Fe^0 in the Fe^0:quartz mixture. The results showed
134 that it is possible to avoid the clogging of the filter by mixing Fe^0 particles with quartz
135 particles. In particular, it was shown that 51 vol-% Fe^0 (25 wt-% when Fe^0 is mixed with
136 quartz) is the critical proportion for with system clogging (porosity loss) will occur upon Fe^0
137 depletion. The present paper attempts to rationalize the admixture of Fe^0 particle with porous
138 particles, including sandstone as used by Leupin et al. [45]. The filling of the total porosity
139 (inter-particles voids and internal porosity) will be considered. The next section will discuss
140 the efficiency of a Fe^0/sand filter.

141 ## 3 Relevant parameters influencing the efficiency of the Fe^0/sand filter

142 ### 3.1 Permeability of granular materials

143 Water permeability is essential for Fe^0/sand filter efficiency because it determines the rate of
144 flow and, thus, the filtration ability. Many models have been proposed to relate the water
145 permeability of granular medium to their microstructure characteristics [50-54]. These models
146 show that permeability is controlled by the packing, shape, sorting (particle size distribution),
147 and porous structure of used granular material, but it appears that porosity and tortuosity of
148 granular materials are two of the primary factors that control water flow process [53-58]. In
149 the most general way, permeability depends on the total porosity which is the ratio of the total
150 volume of voids to the total volume of material. More importantly, however, permeability
151 depends on the way in which the total porosity is distributed and thus on the effective
152 porosity. The effective porosity characterizes the degree to which available pores are
153 interconnected. As a rule, if all pores of a granular material are well interconnected, the total
154 porosity is equal to the effective porosity. Tortuosity can be defined as the ratio of the real

155 length that the water travels inside a filter to the thickness of the filter. For a mixture of non
156 porous particles, the tortuosity can be simply estimated as a function of the total porosity
157 considering the solid grains as spherical inclusions in a fluid phase [59,60].
158 An idealized conventional Fe^0/sand filter is made up of spherical iron and quartz particles of
159 approximately equal diameter. The non porous spherical particles provide ample, unrestricted
160 void spaces that are free from smaller grains and are very well linked. Consequently, a
161 Fe^0/sand filter initially has a high permeability which is related to the total porosity as water
162 flow will occur through the inter-particular voids. In case of using porous particles with
163 poorly interconnected internal voids (as for pumices, ref. [57] and ref. therein), the water
164 permeability is essentially related to the effective porosity due to the inter-particular voids. In
165 this case the tortuosity of the mixing only depends on the effective porosity. Indeed, part of
166 the water may remain apparently stagnant in the internal pores of particles and slowly diffuses
167 out of the pores.

168 **3.2 Efficiency of a Fe^0/sand filter**

169 Due to the expansive nature of iron corrosion the voids are progressively filled by (i) in situ
170 generated iron oxyhydroxides, (ii) immobilized contaminants and (iii) in-situ generated
171 biofilms [12,23,61,62]. The ability to accurately predict the process dependent evolution of
172 the permeability of a Fe^0/sand filter depends on a detailed description of the processes
173 yielding to porosity loss. In this study, the contribution of biofilms and contaminants to
174 porosity loss is not considered. The volumetric expansive nature of iron corrosion is
175 considered as the sole important path. A second simplification is necessary as iron
176 oxyhydroxides are also porous in nature. It is considered that the pores of generated iron
177 oxides are well interconnected. In this case, the filter permeability is solely modified by the
178 process of oxide formation (pore filling). The permeability of a Fe^0/sand filter typically
179 decreases from the beginning of the operation to the time of complete pore filling by iron
180 oxyhydroxides (porosity equal zero).

181 The suitability of Fe^0 as reactive medium for drinking water filters relies on two essential
182 characteristics: (i) the interactions of corroding iron with contaminants (adsorption, co-
183 precipitation/enmeshment, oxidation, reduction), and (ii) the improved size exclusion by
184 virtue of the expansive nature of iron corrosion. The efficiency of an iron filter depends on
185 several factors including particle size of Fe^0, initial contaminant concentration, and influent
186 pH. These factors are determinant to the time at which the initial porosity is reduced to zero.
187 The present discussion will not address how these factors affect Fe^0 reactivity. The evolution
188 of filter permeability due to filling of porosity by iron oxyhydroxides which is the most
189 important parameter determining filter service life will be solely addressed.

190 **3.3 Aim of the paper**

191 Permeability variation in an iron filter is important for predicting filter service life.
192 Understanding the dependence of filter permeability on the extent of iron consumption would
193 be decisive in designing filters. An ideal iron filter is a random pack of identical spheres in a
194 column. The porosity of such an ideal system has a fundamental value of 36 % assuming a
195 compactness of 64 % with soft vibration [30,54-56]. The actual porosity value for a Fe^0/sand
196 filter will depend on the size distribution of filling particles but this porosity is a good
197 approximation for such mixing. As iron consumption progresses, residual Fe^0 particles
198 become compacted and cemented, and the initial porosity (ideally 36 %) progressively
199 decreases down to zero. At porosity zero, the filter is clogged (Figure 1). Cemented Fe^0
200 particles form a continuous frame which had been called “cake”. The described dynamic
201 evolution of the porosity is somewhat equivalent to the formation of quartz (porosity zero)
202 from sandstone (porosity 40 %) by diagenesis [63] (Figure 2).
203 As described above, clogging is inherent to Fe^0 filters working at near neutral pH values
204 (more exactly at pH > 4.0). Therefore, lengthen filter service live initially depends on the
205 ability to create additional space for in-situ generated iron oxyhydroxides while maintaining
206 filter efficiency. An obvious possibility is to use porous material which internal porous

structure may store in-situ generated iron iron oxyhydroxides (Fig. 1) leading to increase the residual effective porosity and thus the residual permeability of the mixing.

4 Efficiency of the Fe^0/sand/porous materials filter

4.1 Background

This work tests the hypothesis, that porous minerals and rocks have the potential to enhance the sustainability of metallic iron (Fe^0) filter. Therefore, it is not important to work with a well-characterized porous material. The concept of "critical porosity" [63] will be used for the discussion. Critical porosity is defined as "the porosity above which the rock can exist only as a suspension". The critical porosity, separates two fundamentally different domains – one of consolidated, frame-supported rocks, and another of fluid-supported suspensions (see ref. [63] for more details). Tab. 2 summarizes the critical porosity value of various rock types. The major feature from Tab. 2 is that the potential exists to find rocks of porosity 0 (quartz) to 80 % (pumice). The highest value from Tab. 2 will be used to qualitatively demonstrate the feasibility of extending filter service live by replacing sand by porous material in a conventional Fe^0/sand filter. Some suitable porous materials are presented in Supporting Information. It can be noticed that the permeability of porous materials is linked to their porous structure (pore connectedness). In general, due to diffusive processes in porous structures, slower kinetics of water flow will be observed comparative to a conventional Fe^0/sand filter. Regardless from the pore connectedness, it is expected that material porosity will effectively store in-situ generated iron oxyhydroxides.

This section presents modelling works to evaluate the feasibility of lengthening the service live of conventional Fe^0/sand filter for safe drinking water by partially or totally substituting sand (quartz) by a porous material. The delay time to filter clogging is evaluated from the evolution of the total residual porosity. Results for pumices are presented and discussed. It can be noticed that the calculus can be made with other porous particles (by changing its

232 critical porosity); the results will be slightly different but the general conclusions will remain
233 identical.

234 **4.2 Design and modelling**

235 A reactive zone (rz) of Fe^0 with a thickness H_{rz} is introduced in the fine sand layer of a
236 conventional biosand filter (Fig. 3) [7,64]. The reference reactive zone is made up of 51 vol-
237 % Fe^0 and 49 vol-% quartz. This system was demonstrated to allow increased filter efficiency
238 compared to a conventional reactive zone with 100 % Fe^0 [30]. The characteristics of the
239 reactive zone are given in Tab. 3. All particles are considered spherical in shape with an
240 average diameter of 1.2 mm. The specific weight of Fe^0 and quartz are ρ_{Fe} = 7800 kg/m^3 and
241 ρ_{sand} = 2650 kg/m^3 respectively. The biosand filter is supposed to work under anoxic
242 conditions. Thus, Fe_3O_4 is the sole iron corrosion product with a coefficient of volumetric
243 expansion η equal to V_{Fe3O4} / V_{Fe} = 2.1.

244 Quartz particles are replaced by porous particles in order to increase the initial total porosity
245 Φ_0 of the reactive zone given by:

246 $$\Phi_0 = \Phi_{0(51\%Fe-49\%Quartz)} + \varphi_{pp} \cdot f_{pp} \qquad (1)$$

247 where the porosity $\Phi_{0\ (51\%FE-49\%sand)}$ = 1 – C. C is the compactness of the granular material (C
248 = 0.64) [54-56] and "1 – C" corresponds to the inter-particular voids (porosity of the mixing
249 without porous particles);

250 φ_{pp} (-) is the critical porosity of the porous particles (e.g. 0.8 for pumice, Tab. 2);

251 f_{pp} (-) is the porous particle volume fraction determined by $f_{pp} = V_{pp}/V$ with V_{pp} the
252 volume of the porous particles and the V the volume of the reactive zone.

253 The filling of the porosity by iron oxyhydroxides can be estimated from a simplified
254 modelling (Figure 1) based on the following assumptions:

255 (i) uniform corrosion: the diameter reduction of the particle is the same for all the Fe particles,

256 (ii) the compactness C and then the initial porosity $\Phi_{0\ (51\%FE-49\%sand)}$ remain constant. The
257 volume of the granular material is not modified by the corrosion process: no pressure induced
258 by rust formation around Fe particles and no compaction of the Fe^0/sand mixture during the
259 corrosion process.
260 (iii) iron oxyhydroxides are fluid enough to progressively fill the available pore space
261 between particles ($\Phi_{0\ (51\%FE-49\%sand)}$) and the porosity of the porous particles. The porous
262 particles are enough close to the iron particles to be filled by the iron oxyhydroxides.
263 Under these assumptions, the residual porosity of the mixing Fe^0-quartz-porous particles is
264 given by:

265 $$\Phi/\Phi_0 = 1 - \frac{N.(\eta-1).4/3.\pi(R0^3 - R^3)}{V.\Phi_0} \quad (2)$$

266 where R_0 (m) is the initial radius of the iron particle, R (m) is the residual radius of the
267 consumed iron particle and η the coefficient of volumetric expansion.
268 The proportion of consumed iron (% consumed Fe) is given by:

269 $$\%\text{consumedFe} = 100.(\frac{R0^3 - R^3}{R0^3}) \quad (3)$$

270 **4.3 Results and discussion for Fe^0/quartz/pumice mixture**

271 The total residual porosity of the mixture Fe^0/quartz/porous particle is given in Tab. 4 and in
272 Fig. 4 and 5. Calculations shown that it is possible to increase the total residual porosity by
273 replacing quartz by porous pumice. For instance, totally substituting quartz by pumice
274 particles having a porosity of 80 % yields to a residual porosity of 41 % when iron is depleted
275 (Tab. 3, Fig. 4). For a given residual porosity (case 1, Fig. 4), more iron is consumed by
276 replacing quartz by pumice. For instance for Φ/Φ_0 = 60 %, the % consumed Fe is about 40 %
277 for 100 % quartz (point A) and 68 % for 100 % pumice (point B). Accordingly, the long-term
278 reactivity of the filter is improved. Furthermore, for a given % consumed Fe, the residual
279 porosity Φ/Φ_0 increases with increasing proportion of pumice. For 68 % consumed Fe^0 (case

280 2), the residual porosity is about 32 % for 100 % quartz (point C) and 60 % for 100 % pumice
281 (point B). The long term permeability of the filter may be improved by up to 45 %.
282 As shown previously, water permeability depends on the effective porosity and not on the
283 total porosity. Some water can remain more or less stagnant in the internal porous structure of
284 a material exhibiting low interconnectivity of pores (or voids). Water flow in the internal
285 porous structure is always slow compared to water flow in the inter-particular voids.
286 Nevertheless the residual effective porosity of the mixture is increased because corrosion iron
287 products are at least partly stored in the porous structure of particles and not totally in the
288 inter-particular voids (see Fig. 1 and 4). Assuming that the porosity of the porous particles
289 (pumice) is totally filled by iron oxyhydroxides, the residual porosity of the inter-particular
290 voids (effective porosity) is 30% leading to better permeability.
291 Experimental studies to validate the efficiency of porous materials to lengthen conventional
292 Fe^0/sand filter service life will consist to evaluate the actual permeability related to the storage
293 of iron oxyhydroxides in porous particles. For instance, 3D imaging by X-ray micro
294 tomography will be an efficient tool to evaluate the residual porosity of the inter-particular
295 voids.

296 **4.4 Generalization: Fe^0/quartz/porous materials**

297 The results discussed above for a pumice exhibiting a porosity of 80 % can be extended to
298 pumices of various porosities and any other porous particles including activated carbons,
299 dolomites, manganese oxides, rock salts, sandstone, and zeolites. Figure 5 depicts the general
300 trend of the results are similar on the sole basis of the porosity (Supporting Information). As a
301 rule, the total residual porosity of the filter increases with increasing particle porosity. For
302 example a material with a grain porosity of 90 % still exhibits 44 % of the initial porosity
303 upon Fe^0 depletion, while a material with a grain porosity of 20 % shows a residual porosity
304 of only 15 %. In practical laboratory experiments, it may be difficult to homogeneously mix
305 materials of very different densities. Remember that the discussion is based on the volumetric

306 filling of the reactive zone by Fe^0 and additives (quartz and porous materials) having the same
307 size. The used mass of individual porous materials should be calculated from tabulated
308 density's values (Tab. 2).
309 Beside the porosity, further physical and chemical properties of individual porous materials
310 should be considered on a case-specific basis. For example, while rocks and activated carbons
311 are inert in water, MnO_{1+x} will be reductively dissolved in Fe^0/sand/H_2O systems. The
312 reductive dissolution of MnO_{1+x} by Fe^{II} (and Fe^0) is necessarily coupled with a volumetric
313 variation (MnO_{1+x} is reduced to MnOOH or dissolved Mn^{II}). However, the discussion of the
314 resulting volumetric variation and its impact on the filter permeability is over the scope of this
315 communication. On the other hand, while using activated carbons as porous additive to
316 sustain filter permeability, the pore size distribution of individual materials should be
317 carefully considered. Remember that porous materials are mainly used as magazine for iron
318 oxyhydroxides. Therefore, mesoporous materials are like more suitable than microporous
319 materials because available pores must be accessible to iron oxyhydroxides.

320 **5 Concluding remarks**

321 The theoretical principles essential to experimentally test the use of porous materials to
322 sustain Fe^0/sand filters are exposed in this study. This approach was rendered possible by
323 revisiting the nature of Fe^0-based filters. It was recalled that a filtration system basically
324 works on the size-exclusion principle [14]. Accordingly, at any time, the pore space must be
325 large enough to enable the expansion/compression cycle inherent to iron corrosion. Iron
326 corrosion products (iron oxyhydroxides) reduce filter porosity and thus permeability while
327 increasing size-exclusion efficiency. The first task to enable long-term iron corrosion was to
328 replace a part of Fe^0 by an inert material (e.g. quartz) [30]. Table 1 clearly shows that the
329 conventional approach of expressing the proportion of Fe^0 by a weight percent is not
330 consistent with the fact that pore volume availability is discussed (expansive nature of iron
331 corrosion). For example, 75 wt-% Fe^0 corresponds to 50.5 vol-% which is almost the

threshold value for which system clogging will occur upon Fe^0 depletion (in a Fe^0:quartz system). In other words, for systems with less than 50.5 vol-% Fe^0, system clogging due to iron corrosion alone is not likely to occur. Moreover, for much lower Fe^0 contents, contaminant breakthrough is likely. Accordingly, some available data are to be re-evaluated. For example, Bi et al. [48] reported on decline in the reactivity of Fe^0 for trichloroethylene reduction when the iron content fell below 50 wt-% (25.4 vol-%; only one halve of the threshold value). The discussion above has shown that this iron content is necessarily insufficient for quantitative contaminant removal.

The present study positively tests the possibility to extend Fe^0 reactivity by replacing quartz by porous materials. Substituting quartz by porous material increased the residual porosity from 0 to 40 % upon Fe^0 depletion. It is expected, that different porous materials (minerals and rocks) will be tested worldwide for use in Fe^0 filters. The option to synthesize porous materials combining permeability and reactivity sustention should be carefully checked for commercial Fe^0 filters. However, the initial goal of this communication is to encourage researchers to improve Fe^0/sand filter efficiency by adding readily available porous material.

Based on the universal availability of both Fe^0 and suitable porous additives, it can be anticipated that the Millennium Development Goal of halving "by 2015 the proportion of people without sustainable access to safe drinking water" can still be achieved [65].

Supporting Information

Selected suitable porous materials to sustain Fe^0/sand filters (8 pages)

Acknowledgments

Dipl.-Geol. Manuela Morales Demarco (Geoscience Centre of the University of Göttingen) is gratefully acknowledged for the insightful discussion on the porosity of rocks and minerals. Sven Hellbach (student research assistant) is acknowledged for technical assistance. The manuscript was improved by the insightful comments of anonymous reviewers from Chemical Engineering Journal.

References

[1] M. Wegmann, B. Michen, T. Luxbacher, J. Fritsch, T. Graule, Modification of ceramic microfilters with colloidal zirconia to promote the adsorption of viruses from water, Water Res. 42 (2008), 1726–1734.

[2] A.H. Malik, Z.M. Khan, Q. Mahmood, S. Nasreen, Z.A. Bhatti, Perspectives of low cost arsenic remediation of drinking water in Pakistan and other countries, J. Hazard. Mater. 168 (2009), 1–12.

[3] S. Wang, Y. Peng, Natural zeolites as effective adsorbents in water and wastewater treatment, Chem. Eng. J. 156 (2010), 11–24.

[4] M.W. LeChevallier, K.K. Au, *Water treatment and pathogen control: process efficiency in achieving safe drinking water*. Geneva, Switzerland: WHO, 2004, http://www.cepis.ops-oms.org/bvsacg/e/cd-cagua/guias/c.referencias/10.watreatpath.pdf (Access 06.06.2010).

[5] M.A. Shannon, P.W. Bohn, M. Elimelech, J.G. Georgiadis, B.J. Marinas, A.M. Mayes, Science and technology for water purification in the coming decades Nature 452, 301–310.

[6] M.D. Sobsey, C.E. Stauber, L.M. Casanova, J.M. Brown, M.A. Elliott, Point of use household drinking water filtration: A practical, effective solution for providing sustained access to safe drinking water in the developing world. Environ. Sci. Technol. 42 (2008), 4261–4267.

[7] CAWST (2009), The Centre for Affordable Water and Sanitation Technology http://www.cawst.org/ (Access 07.06.2010).

[8] M.I. Litter, M.E. Morgada, J. Bundschuh, Possible treatments for arsenic removal in Latin American waters for human consumption, Environ. Pollut. 158 (2010), 1105–1118.

[9] WHO/UNICEF 2010. Progress on sanitation and drinking-water 2010 update, Geneva, Switzerland: WHO/UNICEF. http://www.unwater.org/downloads/JMP_report_2010.pdf (Access 06.06.2010).

384 [10] L. Leong, Removal and inactivation of viruses by treatment processes for potable water
385 and wastewater – a review, Water Sci. Technol. 15 (1983), 91–114.
386 [11] S. Madaeni, The application of membrane technology for water disinfection, Water Res.
387 33 (1999), 301–308.
388 [12] A. Zularisam, A. Ismail, R. Salim, Behaviours of natural organic matter in membrane
389 filtration for surface water treatment – a review, Desalination 194 (2006), 211–231.
390 [13] S. Ahamed, A.K.M. Munir, A. Hussam, Groundwater arsenic removal technologies
391 based on sorbents: Field applications and sustainability, In Handbook of Water Quality
392 and Water Purity, Elsevier Inc., Chapter 16 (2009), 379–417.
393 [14] C. Noubactep, A. Schöner, P. Woafo, Metallic iron filters for universal access to safe
394 drinking water, Clean 37 (2009), 930–937.
395 [15] A.M. Gottinger, D.J. Wild, D. McMartin, B. Moldovan, D. Wang, Development of an
396 iron-amended biofilter for removal of arsenic from rural Canadian prairie potable water,
397 (2010) Retrieved from: http://www.mainstreamwater.com/Gottinger%20et%20al.pdf.
398 (Acces 22.04.2010).
399 [16] D. Mohan, C.U. Pittman Jr., Arsenic removal from water/wastewater using adsorbents –
400 A critical review, J. Hazard. Mater. 142 (2007), 1–53.
401 [17] V.K. Gupta, Suhas, Application of low-cost adsorbents for dye removal – A review. J.
402 Environ. Manag. 90 (2009), 2313–2342.
403 [18] A.D. Henderson, A.H. Demond, Long-term performance of zero-valent iron permeable
404 reactive barriers: a critical review, Environ. Eng. Sci. 24 (2007), 401–423.
405 [19] C. Noubactep, Processes of contaminant removal in "Fe^0–H_2O" systems revisited. The
406 importance of co-precipitation, Open Environ. J. 1 (2007), 9–13.
407 [20] C. Noubactep, A critical review on the mechanism of contaminant removal in Fe^0–H_2O
408 systems, Environ. Technol. 29 (2008), 909–920.

409 [21] C. Noubactep, The suitability of metallic iron for environmental remediation, Environ.
410 Progr. (2009), doi: 10.1002/ep.10406.
411 [22] C. Noubactep, P. Woafo, Elemental iron (Fe^0) for better drinking water in rural areas of
412 developing countries, In Merkel B.J., Hasche-Berger A. (Eds.) *Uranium in the*
413 *Environment*. Springer, Berlin, Heidelberg; (2008), 121–130.
414 [23] V. Zolla, F.S. Freyria, R. Sethi, A. Di Molfetta, Hydrogeochemical and biological
415 processes affecting the long-term performance of an iron-based permeable reactive
416 barrier, J. Environ. Qual. 38 (2009), 897–908.
417 [24] S. Goldberg, Influence of Soil Solution Salinity on Molybdenum Adsorption by Soils,
418 Soil Sci. 174 (2009), 9–13.
419 [25] Hanna, Sorption of two aromatic acids to iron oxides: Experimental study and modeling,
420 J. Colloid Interf. Sci. 309 (2007), 419–428.
421 [26] K. Bhargava, A.K. Ghosh, Y. Mori, S. Ramanujam, Model for cover cracking due to
422 rebar corrosion in RC structures, Eng. Struct. 28 (2006), 1093–1109.
423 [27] T. El. Maaddawy, K. Soudki, A model for prediction of time from corrosion initiation to
424 corrosion cracking, Cem. Concr. Compos. 29 (2007), 168–175.
425 [28] S. Caré, Q.T. Nguyen, V. L'Hostis, Y. Berthaud, Mechanical properties of the rust layer
426 induced by impressed current method in reinforced mortar, Cement Concrete Res. 38
427 (2008), 1079–1091.
428 [29] S. Caré, Q.T. Nguyen, K. Beddiar, Y. Berthaud, Times to cracking in reinforced mortar
429 beams subjected to accelerated corrosion tests, Mater. Struct. 43 (2010), 107–124.
430 [22] C. Noubactep, S. Caré, F. Togue Kamga, A. Schöner, P. Woafo, Extending service life of
431 household water filters by mixing metallic iron with sand, Clean (2010) (Submitted -
432 clen.201000177).

433 [31] A.H. Khan, S.B. Rasul, A.K.M. Munir, M. Habibuddowla, M. Alauddin, S.S. Newaz, A.
434 Hussam, Appraisal of a simple arsenic removal method for groundwater of Bangladesh.
435 J. Environ. Sci. Health A35 (2000), 1021–1041.
436 [32] T.K.K. Ngai, S. Murcott, R.R. Shrestha, B. Dangol, M. Maharjan, Development and
437 dissemination of Kanchan™ Arsenic Filter in rural Nepal, Water Sci. Technol. Water
438 Supply 6 (2006), 137–146.
439 [33] A. Hussam, A.K.M. Munir, A simple and effective arsenic filter based on composite iron
440 matrix: Development and deployment studies for groundwater of Bangladesh, J.
441 Environ. Sci. Health A 42 (2007), 1869–1878.
442 [34] T.K.K. Ngai, R.R. Shrestha, B. Dangol, M. Maharjan, S.E. Murcott, Design for
443 sustainable development – Household drinking water filter for arsenic and pathogen
444 treatment in Nepal, J. Environ. Sci. Health A42 (2007), 1879–1888.
445 [35] D. Pokhrel, B.S. Bhandari, T. Viraraghavan, Arsenic contamination of groundwater in
446 the Terai region of Nepal: An overview of health concerns and treatment options,
447 Environ. Int. 35 (2009), 157–161.
448 [36] A. Neku, N. Tandulkar, An overview of arsenic contamination in groundwater of Nepal
449 and its removal at household level, J. Phys. IV (2003), 941–944.
450 [37] A. Hussam, Contending with a Development Disaster: SONO Filters Remove Arsenic
451 from Well Water in Bangladesh, Innovations 4 (2009), 89–102.
452 [38] H.-M. Hung, F.H. Ling, M.R. Hoffmann, Kinetics and mechanism of the enhanced
453 reductive degradation of nitrobenzene by elemental iron in the presence of ultrasound,
454 Environ. Sci. Technol. 34 (2000) 1758–1763.
455 [39] H. Zhang, M. Jiang, Z. Wang, F. Wu, Decolorisation of CI Reactive Black 8 by zero-
456 valent iron powder with/without ultrasonic irradiation. Color. Technol. 123 (2007) 203–
457 208.

458 [40] P. G. Tratneyk, Putting corrosion to use: Remediating contaminated groundwater with
459 zero-valent metals, Chemistry & Industry 1 July (1996) 499–503.
460 [41] S.F. O´Hannesin, R.W. Gillham, Long-term performance of an in situ "iron wall" for
461 remediation of VOCs, Ground Water 36 (1998), 164–170.
462 [42] P. Westerhoff, J. James, Nitrate removal in zero-valent iron packed columns, Wat. Res.
463 37 (2003) 1818–1830.
464 [43] D.I. Kaplan, T.J. Gilmore, Zero-valent iron removal rates of aqueous Cr(VI) measured
465 under flow conditions, Water Air Soil pollut. 155 (2004), 21–33.
466 [44] O.X. Leupin, S.J. Hug, Oxidation and removal of arsenic (III) from aerated groundwater
467 by filtration through sand and zero-valent iron, Wat. Res. 39 (2005) 1729–740.
468 [45] O.X. Leupin, S.J. Hug, A.B.M. Badruzzaman, Arsenic removal from Bangladesh tube
469 well water with filter columns containing zerovalent iron filings and sand, Environ. Sci.
470 Technol. 39 (2005) 8032–8037.
471 [46] H.-L. Lien, R.T. Wilkin, High-level arsenite removal from groundwater by zero-valent
472 iron. Chemosphere 59 (2005) 377–386.
473 [47] P. Westerhoff, M. DeHaan, A. Martindale, M. Badruzzaman, Arsenic adsorptive media
474 technology selection strategies. Water Quality Res. J. Canada 41 (2006) 171–184.
475 [48] E. Bi, J.F. Devlin, B. Huang, Effects of mixing granular iron with sand on the kinetics of
476 trichloroethylene reduction, Ground Water Monit. Remed. 29 (2009), 56–62.
477 [49] A.M. Gottinger, Chemical-free arsenic removal from potable water with a ZVI-amended
478 biofilter. Master thesis, University of Regina (Saskatchewan, Canada) (2010) 90 pp.
479 [50] G.V. Chilingar, Relationship between porosity, permeability, and grain-size distribution
480 of sands and sandstones. Develop. Sediment. 1 (1964), 71–75.
481 [51] W. Wempe, G. Mavko, Three distinct porosity domains defined physically,
482 hydraulically, electrically, and elastically, The Leading Edge 17 (2001), 198–199.

[52] L.C.M. Félix, L.A.B. Muñoz, Representing a relation between porosity and permeability based on inductive rules, J. Petrol. Sci. Eng. 47 (2005), 23–34.

[53] S.-H. Lee, H.Y. Jo, S.-T. Yun, Y.J. Lee, Evaluation of factors affecting performance of a zeolitic rock barrier to remove zinc from water, J. Hazard. Mater. 175 (2010), 224–234.

[54] E. Zaman, P. Jalali, On hydraulic permeability of random packs of monodisperse spheres: Direct flow simulations versus correlations. Physica A389 (2010), 205–214.

[55] D.J. Cumberland, R.J. Crawford, *Handbook of powder technology. The packing of particle* Vol. 6, J.C. Williams & T. Allen, Elsiever, Amsterdam (**1987**).

[56] F. de Larrard, *Granular structure and formulation of concretes* (in French), Etudes et recherches des Laboratoires des ponts et chaussées 34, Laboratoire central des ponts et chaussées, Paris (**1999**), 414 pp.

[57] P.W. Reimus, T.J. Callahan, S.D. Ware, M.J. Haga, D.A. Counce, Matrix diffusion coefficients in volcanic rocks at the Nevada test site: Influence of matrix porosity, matrix permeability, and fracture coating minerals. J. Contam. Hydrol. 93 (2007), 85–95.

[58] M. Nakamura, K. Otaki, S. Takeuchi, Permeability and pore-connectivity variation of pumices from a single pyroclastic flow eruption: Implications for partial fragmentation. J. Volcanol. Geoth. Res. 176 (2008), 302–314.

[59] S. Caré, Aggregate influence on chloride ion diffusion into mortar, Cement Concrete Res. 33 (2003) 1021–1028.

[60] S. Caré, E. Hervé, Application of n-phase model to the diffusion coefficient of chloride in mortar, Transp. Porous Media 2 (August 2004) 119–135.

[61] M.M. Scherer, S. Richter, R.L. Valentine, P.J.J. Alvarez, Chemistry and microbiology of permeable reactive barriers for in situ ground water cleanup, Crit. Rev. Environ. Sci. Technol. 30 (2000), 363–411.

508 [62] M. Shafahi, K. Vafai, Biofilm affected characteristics of porous structures, Int. J. Heat
509 Mass Trans. 52, (2009), 574–581.
510 [63] A. Nur, G. Mavko, J. Dvorkin, D. Galmudi, Critical porosity; a key to relating physical
511 properties to porosity in rocks. The Leading Edge 17 (1998), 357–362.
512 [64] M. Lea, Biological sand filters: low-cost bioremediation technique for production of
513 clean drinking water, Curr. Prot. Microbiol. (2008) 1G.1.1-1G.1.28.
514 [65] WHO, Guidelines for Drinking-water Quality, Recommendations, 3rd ed.; World Health
515 Organization: Geneva, 2006; Vol. 1.
516

516 **Table 1**: Overview on the objectives of using iron/sand mixtures and relationship between
517 percent iron mass (wt-%) and percent iron volume (vol-%). The conventional
518 expression of the iron amount (wt-%) does not directly accounts for the expansive
519 nature of iron corrosion. For example the often used 1:1 (50 wt-% Fe^0)
520 corresponds to 25.4 vol-% Fe^0. Filter or column clogging due to iron corrosion
521 alone will not occur (threshold value 51 vol-% Fe^0).
522

Iron (wt-%)	**Iron** (kg)	**Sand** (kg)	**Iron** (vol-%)	**Scale**	**Objective**	**Ref.**
22	6100	21500	8.8	pilot study	sustained permeability	[31]
20	0.60	2.40	7.8			
50	1.50	1.50	25.4	lab columns	sustained reactivity	[33]
100	3.00	0.00	100.0			
25	0.02	0.06	10.2			
50	0.04	0.04	25.4			
75	0.06	0.02	50.5	lab columns	Fe^0 cost reduction	[37]
85	0.07	0.01	65.8			
100	0.08	0.00	100.0			

523
524
525

525 **Table 2:** Density and critical porosity of selected potential additives for improved reactivity
526 of conventional Fe^0 filters. All critical porosity's values for rocks are from Nur et al.
527 [63]. The value for activated carbon is an indicative average value from the
528 literature.
529

Material	**Density** (g/cm^3)	**Average Density** (g/cm^3)	**Critical Porosity** (%)
Quartz	2.65	-	0
Sandstone	2.2 - 2.8	2.50	40
Limestone	2.3 - 2.7	2.50	40
Dolomites	2.8 - 2.9	2.85	40
Pumice	0.36-0.91	0.64	80
Chalks	1.8-2.6	2.20	65
Rock Salts	2.5 - 2.6	2.55	40
Oceanic Basalts	2.8 - 3.0	2.90	20
Activated carbons	0.44-2.50	1.47	55

530
531

Table 3: Composition and thickness (H_{rz}) of the reactive zone for 3 kg of Fe^0. Fe^0 and sand particles are 1.2 mm in diameter. The value C = 0.64 is considered for compactness. The residual porosity $\Phi/\Phi_0 = 0$ is obtained for 100 % consumed Fe.

$[Fe^0]_0$ (vol-%)	$[Fe^0]_0$ (kg)	$[sand]_0$ (kg)	H_{rz} (cm)	Φ/Φ_0 (-)	$[Fe^0]_\infty$ (%)	$[Fe^0]_\infty$ (kg)
51	3.00	0.98	1.67	0.0	0.00	0.00

536 **Table 4**: Composition of the reactive zone for 51% Fe^0 (3 kg of Fe^0) and 49 % of additive
537 particles (quartz or porous materials). Fe^0 and additives particles are 1.2 mm in
538 diameter. The residual porosity $\Phi/\Phi_0 = 0$ is given for 100 % consumed Fe. The
539 value C = 0.64 is considered for compactness. The thickness H_{rz} of the reactive zone
540 is 1.67 cm. The specific weight and the critical porosity of pumice are respectively
541 $\rho_{Pumice} = 640$ kg/m^3 and $\varphi_{pumice} = 0.8$ (-).

542

Pumice (%)	Fe^0 (kg)	Quartz (kg)	Pumice (kg)	Φ_0 (-)	Φ/Φ_0 (-)
0	3	0.98	0.00	0.36	0.00
10	3	0.88	0.02	0.39	0.07
20	3	0.78	0.05	0.41	0.12
30	3	0.69	0.07	0.44	0.18
40	3	0.59	0.09	0.46	0.22
50	3	0.49	0.12	0.49	0.26
60	3	0.39	0.14	0.51	0.30
70	3	0.29	0.17	0.54	0.33
80	3	0.20	0.19	0.56	0.36
90	3	0.10	0.21	0.59	0.39
100	3	0.00	0.24	0.61	0.41

543

544

544 Figure 1

545

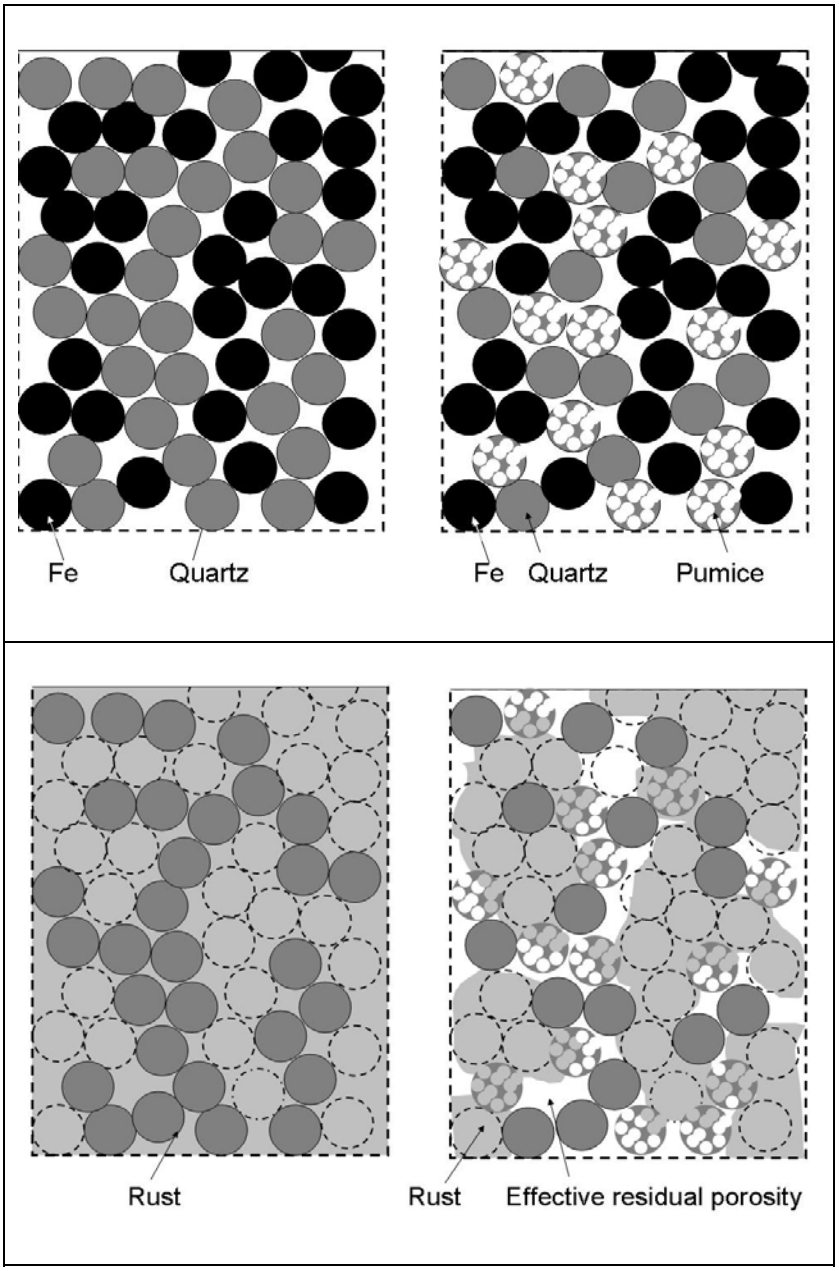

546

547

547 **Figure 2**

548

Figure 2: Schematic diagrams showing the evolution of the porous structure during the diagenesis of quartz. As diagenesis progresses. sand grains become compacted and cemented. The initial porosity (40 %) decreases down to zero. Modified after Nur et al. [63].

549

550

Figure 3

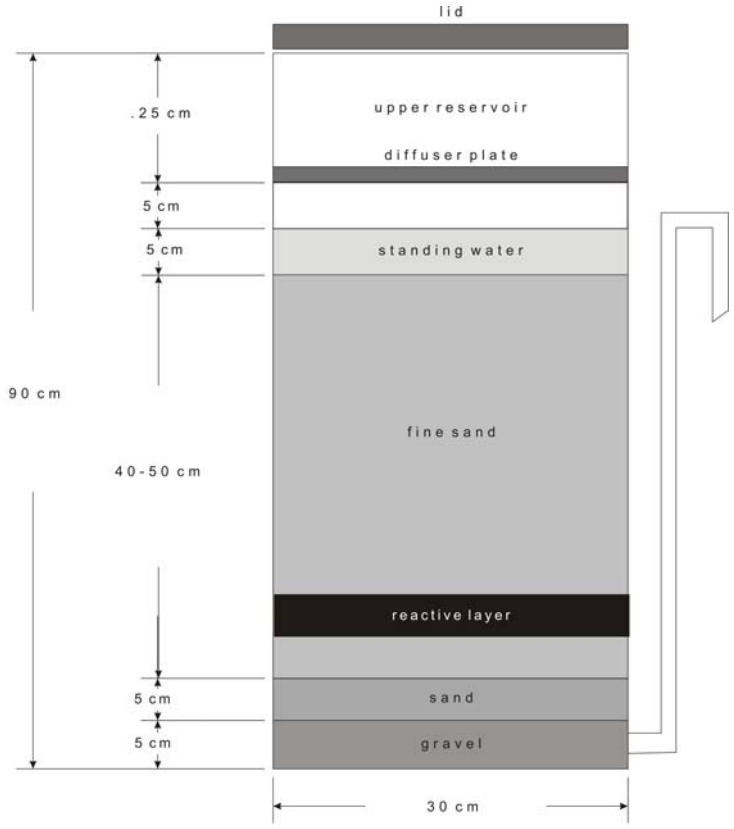
lid
.25 cm
upper reservoir
diffuser plate
5 cm
5 cm
standing water
90 cm
fine sand
40-50 cm
reactive layer
5 cm
sand
5 cm
gravel
30 cm

553 **Figure 4**

554

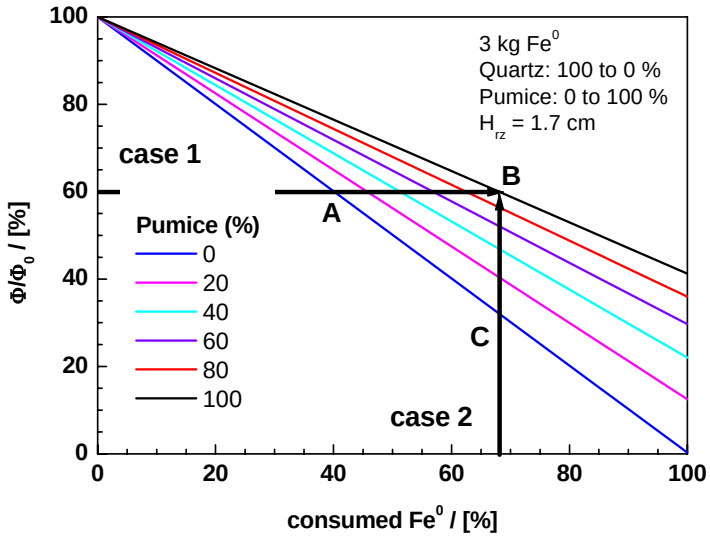

555

556

557

558

Figure 5

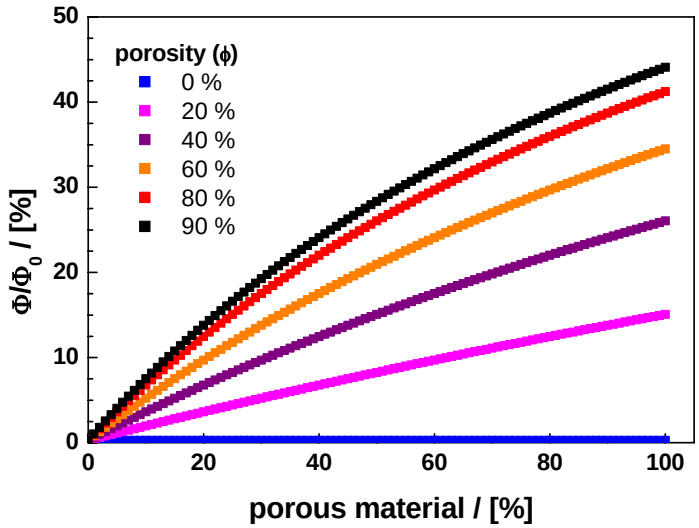
porosity (ϕ)
0 %
20 %
40 %
60 %
80 %
90 %
Φ/Φ0 / [%]
porous material / [%]
0
10
20
30
40
50
0
20
40
60
80
100

Figure captions

Figure 1: Schematic diagrams showing the extend of porosity loss as influenced by the substitution of a part of sand by a porous material: initial stage (top) and final stage (down). The final stage corresponds to Fe^0 depletion (100 % consumption). At Fe^0 depletion, the residual porosity is zero for the conventional Fe^0/sand filter. The effective residual porosity is increased for Fe^0/sand/pumice filter (see text).

Figure 2: Schematic diagrams showing the evolution of the porous structure during the diagenesis of quartz. As diagenesis progresses, sand grains become compacted and cemented. The initial porosity (40 %) decreases down to zero. Modified after ref. [63].

Figure 3: Schematic diagram of an iron-reactive-zone containing Biosand filter. The illustration highlights major principles and generic size dimensions. Modified after ref [64]. The thickness of a reactive layer containing 3 kg Fe^0 representing 51 % (vol.) of the filling is 1.67 cm (see Tab. 3).

Figure 4: Evolution of the residual porosity Φ/Φ_0 versus the % consumed Fe for 51% Fe^0 (3 kg of Fe^0) and 49% of quartz/pumice particles. Fe^0 and quartz/pumice are 1.2 mm in diameter. The %consumed Fe is given by $\%\text{consumedFe} = 100.\left(\frac{R0^3 - R^3}{R0^3}\right)$ with R_0 the initial radius of Fe^0 and R the residual radius. The value C = 0.64 is considered for compactness. The thickness H_{rz} of the reactive zone is 1.67 cm. The specific weight and the critical porosity of pumice are respectively ρ_{Pumice} =640 kg/m^3 and φ_{pumice} =0.8 (-).

Figure 5: Evolution of the residual porosity Φ/Φ_0 versus the %replaced quartz particles for 51 % Fe^0 (3 kg of Fe^0) and 49 % of quartz/porous particles. Fe^0 and additives are 1.2 mm in diameter. The residual porosity $\Phi/\Phi_0 = 0$ is given for 100 % consumed Fe for various porous particles with porosity φ_{pp}. The value C = 0.64 is considered for compactness. The thickness H_{rz} of the reactive zone is 1.67 cm.